Key Engineering Materials
ISSN: 1662-9795, Vol. 1048, pp 165-177
doi:10.4028/p-wC1Lah

Submitted: 2026-01-20
Revised: 2026-02-12
Accepted: 2026-02-27
Online: 2026-04-14

Numerical Data-Driven Modelling of Modified Samanta Process for Cold Extrusion of Gears

Tahsin Deliktas[1,a*], Marcel Görz[1,b], Adrian Schenek[1,c], Marco Speth[1,d], Mathias Liewald[1,e]

[1]University of Stuttgart, Institute for Metal Forming Technology (IFU), Holzgartenstraße 17, 70174 Stuttgart, Germany

[a*]tahsin.deliktas@ifu.uni-stuttgart.de, [b]marcel.goerz@ifu.uni-stuttgart.de, [c]adrian.schenek@ifu.uni-stuttgart.de, [d]marco.speth@ifu.uni-stuttgart.de, [e]mathias.liewald@ifu.uni-stuttgart.de
(*corresponding author)

Keywords: Metal Forming, Cold Forging, Gears, Simulation, Machine Learning

Abstract. The Guided Material Flow (GMF) process is an advanced variant of the Samanta process designed for the net shape cold extrusion of gears. The GMF process employs a modified die geometry to control material flow and significantly reduce maximum tool loads, effectively overcoming traditional process limitations. Key advantages include enhanced tooth tip strength and a reduction in face end deformations, which are characteristic defects in the conventional Samanta process. Minimising these deformations reduces the requirement for subsequent machining and enhances overall material efficiency. A numerical dataset was generated to train and validate data driven surrogate models, facilitating rapid process analysis without the computational cost of continuous Finite Element Analysis (FEA). The models developed in this paper enable the precise prediction of critical process outputs, including maximum punch force, die filling behaviour, material utilisation and strain hardening at the tooth tip. This paper details the numerical data acquisition, the specific training and validation methodologies of the machine learning models and demonstrates their capability to accurately predict complex process outcomes when varying the geometry of the die active surface in the GMF process.

Introduction

The demand for high performance gears for industrial applications continues to drive the development of resource-efficient manufacturing processes. Cold forging, and cold extrusion in particular, offers significant advantages over conventional machining, including high material utilisation, superior surface quality and increased strength of component due to strain hardening [1]. For this reason, numerical and experimental investigations into the prediction of material flow and tool loads have been essential for enhancing process reliability in gear forging [2–7]. Within this field, the Samanta process represents a special cold extrusion process for gear manufacturing. Its characteristic operating principle consists of extruding full or hollow blanks partially into a splined die without ejection. After the punch is retracted, a subsequent blank is inserted, which then presses the previously partially formed blank completely through the splined die to obtain the finished gear [8–10]. However, the industrial application of the conventional Samanta process is limited by several technological challenges. In particular, high tool loads, limited gear accuracy and characteristic material deformations at the face ends often necessitate subsequent machining, thereby reducing overall material efficiency [8, 11]. In order to address these challenges, a modified variant of the Samanta process, the so-called Guided Material Flow (GMF) process, was developed and previously investigated by the authors [12, 13]. The GMF approach fundamentally differs from the conventional Samanta process through a redesigned active die surface, which significantly alters the material flow and the resulting stress state within the deformation zone. As illustrated in Fig. 1, this modified die geometry is characterised by three primary features: 1. an elongated forming zone, 2. a taper of the tooth cavity, and 3. an undercut of the cavity at the tooth tip area. The elongated forming zone distributes deformation work to reduce peak punch forces and improve gear precision. Although such

elongation may compromise tooth filling, the tapered cavity geometry generates tangential compressive stresses to prevent material flow in a radial inward direction. Furthermore, the undercut compensates for increased friction and enhances strain hardening through pronounced local plastic deformation.

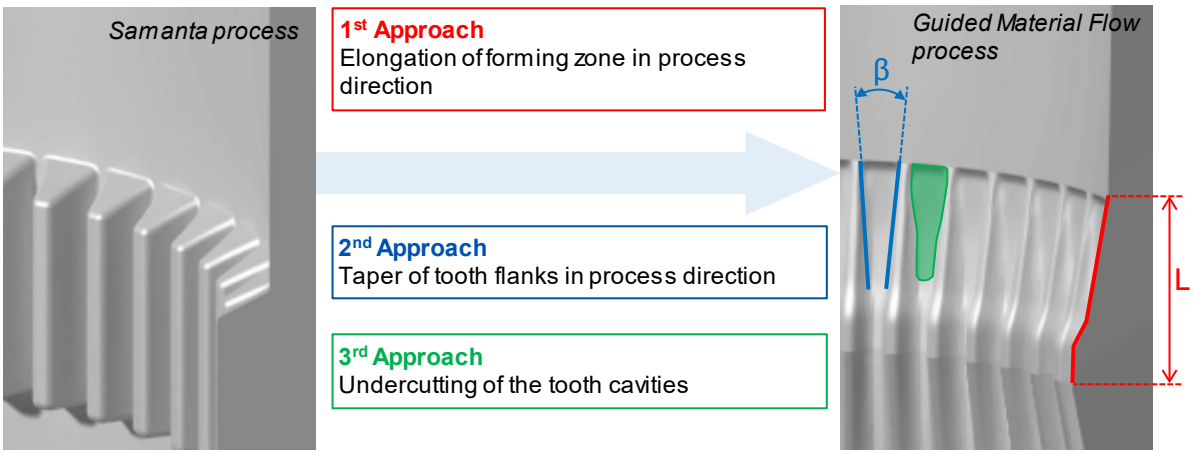

Fig. 1. Modifications of active die surface in the GMF process compared to the Samanta process

Previous studies on the GMF process demonstrated that the modified die geometry effectively reduces tool loads while improving material flow in the tooth cavity. In these investigations, the finite element model was successfully validated against experimental cold extrusion tests using novel GMF die active surfaces, where numerical results showed excellent agreement with physical test data [12]. Even though these die active surfaces have since been iteratively modified and further optimised, the initial validation remains the scientific foundation for the identified correlations between die geometry and process outputs.

However, there is a highly non-linear correlation between changes to the active die surface and the process outputs. The complex interdependencies between the various geometric parameters and process outputs, such as punch force and die filling, require a more sophisticated approach for optimisation, as the effectiveness of surrogate models for such data-driven analyses has already been demonstrated by Schenek [14] for sheet metal stamping processes. Relying on a full factorial design of experiments (DOE) based on 3D Finite Element Analysis (FEA) simulations is prohibitively time-consuming and cost-intensive, which prevents a comprehensive exploration of the design space.

Addressing these computational limitations, this paper presents a data driven surrogate modelling approach. By using Machine Learning algorithms and integrating data normalisation, which accounts for the scaling laws of gear geometry based on gear module m, a precise predictive model is developed. The python-based framework enables the rapid prediction of process loads, strain hardening at the tooth tip, tooth filling and material utilisation, thereby providing a foundation for automated optimisation of the GMF process.

Numerical Data Acquisition

The generation of a high-quality dataset of a manufacturing technology stands for a fundamental step for developing corresponding data-driven models. This chapter details the methodology used to acquire the numerical data for the GMF process. It covers the revision of the tool geometry, the definition of the numerical boundary conditions in DEFORM-3D™ and the systematic exploration of the parameter space. By combining advanced FEA with a structured sampling strategy, a comprehensive database is established to capture the complex interactions between tool design and process outputs.

Tool Design and Process Setup. The design of the die in the GMF process has been established in previous studies [12, 13]. In this work, the model was refined by revising the shoulder geometry. While earlier investigations utilised linear, quadratic and cubic functions to realise shoulder geometries, it was found that the cubic variant offered no significant advantages. Consequently, the

shoulder geometry in the current model is defined by a single radius R_s. For the subsequent data processing and model training, this geometric parameter is transformed into a standardised factor, hereafter referred to as the *R-factor*. This factor is defined as the scaled curvature of the shoulder:

$$R - factor = \frac{1}{R_s} \cdot 1000 \quad (1)$$

This mathematical transformation serves two primary purposes. First, using the inverse of the radius eliminates the numerical singularity of a linear shoulder geometry ($R_s \rightarrow \infty$) by representing it as a curvature of zero. This enables a continuous parameter space where the sign determines the curvature direction. As Fig. 2b illustrates, a positive *R-factor* defines a concave shoulder design, while a negative value results in a convex geometry.

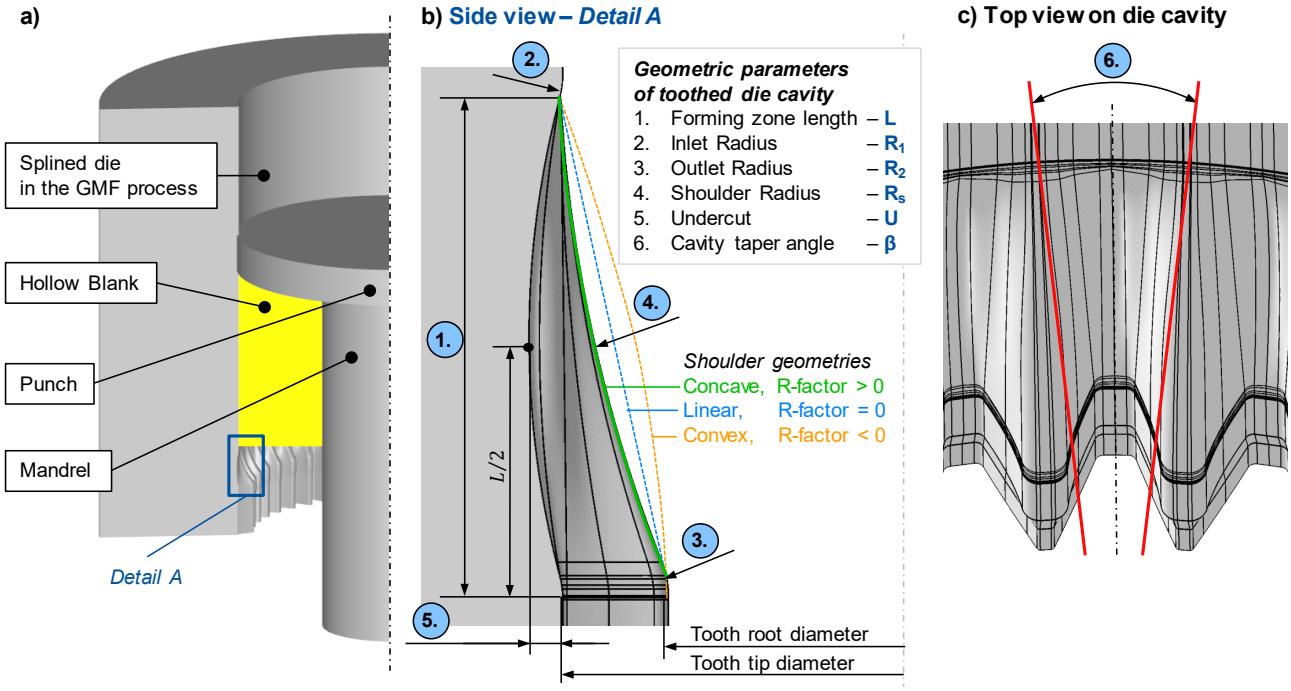

Fig. 2. GMF process, (a) process setup in DEFORM 3D™; (b) side view; (c) top view on die cavity.

Second, the scaling factor of 1.000 aligns the magnitude of the curvature values with the other geometric parameters, ensuring balanced feature weighting for the data-driven models. Beyond the shoulder geometry, the study investigates additional geometric variables shown in Fig. 2b and Fig. 2c. These include the axial length of the forming zone L together with the taper angle of the cavity β. Furthermore, the transition radii leading to the shoulder and the calibration zone, denoted as R_1 and R_2, as well as the magnitude of the undercut U, constitute the key variables for this investigation.

Validation of Numerical Simplifications. The numerical process mapping is shown in Fig. 2a. This model is based on the Samanta principle, which inherently operates without the need for ejectors. Although the physical process typically involves extrusion in a stacked package, the numerical setup was simplified to the direct extrusion of a single workpiece. Both numerical setups are shown in Fig. 3a. The simulation of the stacked process variant requires the modelling of three consecutive strokes. This results in the complete forming of two workpieces, while a third remains partially formed within the die cavity. To ensure a valid steady-state analysis, the evaluation of the stacked simulation is performed specifically on the second workpiece in sequence. Furthermore, all simulations in this study were performed using a half-tooth segment of the respective gear geometry to exploit symmetry and reduce calculation time. For this numerical comparative analysis, a gear with a module of $m = 1$ mm and a number of teeth $z = 39$ was selected, using the material 16MnCrS5 (modelled as ideally plastic). In all simulation variants, the workpieces were defined with a constant height of 25 mm. The GMF die for this comparison was defined with a random geometric configuration of the functional surface ($L = 10$ mm, $U = 0.2$ mm, etc.). The extended punch force

curve and the resulting larger stroke for the GMF process in Fig. 3b result from the elongated forming zone, which represents an intended effect to lower the maximum punch force.

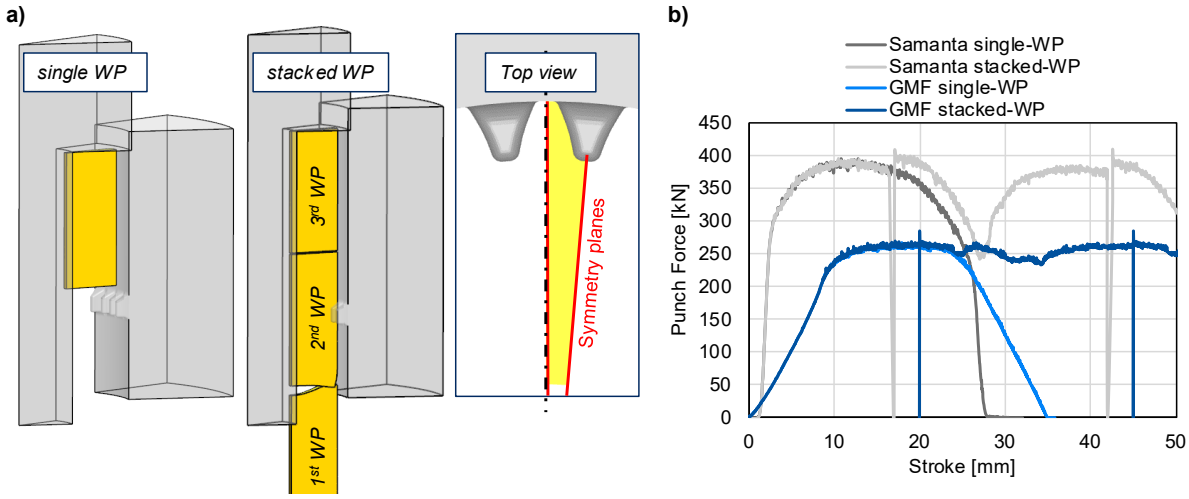

Fig. 3. Numerical analysis of single and stacked process, (a) numerical setups; (b) punch force calculation.

The reduction of the model complexity to a single-workpiece setup was chosen to mitigate computational costs and contact-related instabilities associated with modelling multiple interacting workpieces, following a methodological simplification previously utilised by Kiener et al. [7]. To verify these assumptions, comparative simulations between the single-workpiece model and the full-package process were performed using the same numerical setup as described in the subsequent sections. It was shown that this approach does not affect the maximum punch force (see Fig. 3b), the material flow within the cavity or the stress-strain state within the forming zone during stationary process phases.

The model simplification primarily affects the face end deformations, as compared in Fig. 4 for the Samanta and GMF processes using a single workpiece (WP) and stacked workpieces setups. In the Samanta process, the differences between the two setups are minimal. The face end deformation in the single workpiece variant amounts by 0.43 mm higher, while the tooth filling remains nearly identical. Consequently, after machining the defective workpiece volume, both Samanta variants result in an almost identical net gear height Δh.

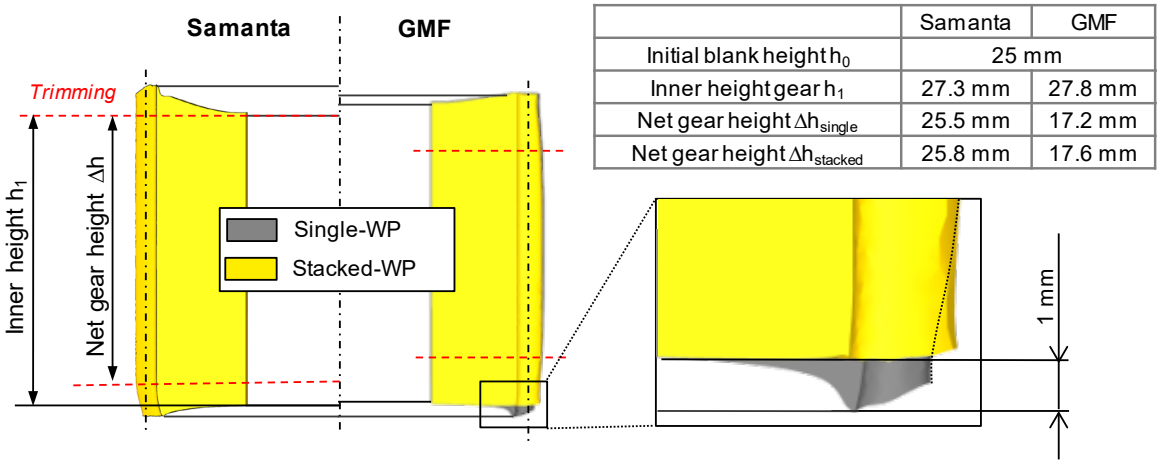

	Samanta	GMF
Initial blank height h_0	25 mm	
Inner height gear h_1	27.3 mm	27.8 mm
Net gear height Δh_{single}	25.5 mm	17.2 mm
Net gear height $\Delta h_{stacked}$	25.8 mm	17.6 mm

Fig. 4. Numerical evaluation of net gear height: Comparison between single and stacked workpieces (WP) for the Samanta and GMF processes.

The GMF process using the single workpiece model shows that the deformations at the bottom of the workpiece are slightly more pronounced compared to the stacked workpiece model. This is due to the lack of axial counter-pressure in the single workpiece variant, which is otherwise provided by the partially formed workpiece already present in the die. Consequently, this absence of resistance results also in a different characteristic of the tooth filling, as seen in the detail view in Fig. 4. In

contrast, deformation and mold filling on the top side of the workpiece remain nearly identical in both variants. After the numerical removal of underfilled material sections, a minor difference in net gear height is observed, decreasing from 17.6 mm (stacked WP) to 17.2 mm (single WP). Due to this small deviation, the simplification of the process sequence for the GMF process is considered valid and is therefore utilised for the further investigations.

Regarding the comparison between the Samanta and newly developed GMF processes, the differences in net gear height observed in this study are primarily a result of the non-optimised, exemplary die configuration selected for the GMF process.

Numerical Setup in DEFORM-3D™. Numerical simulations were performed using the commercial FE software DEFORM-3D™ . To improve computational efficiency while maintaining high calculation accuracy, the GMF process was modelled as hollow forward extrusion (as shown in Fig. 2a). This configuration reduces the workpiece volume without affecting the material flow in the splined forming zone, punch force or the stress-strain state in the forming zone compared to a full workpiece. Due to the symmetry of the gear geometry, the simulation was limited to a half-tooth segment. The initial height of the workpiece section was 25 mm. The case-hardening steel 16MnCrS5 was selected as the workpiece material for this investigation. To accurately represent the material behavior, flow curves experimentally determined via the Gleeble 3800C thermomechanical simulator at strain rates of 0.1, 1 and 10 s^{-1} for temperatures of 20, 100, 200, 300 and 400 °C were implemented into the FE software. The workpiece was modelled using an ideal plastic material law to reduce calculation time. Since tool loads are directly linked to the punch force, an analysis of elastic die expansion will be conducted in future studies focusing on load optimised GMF die geometries. The kinematics were defined by a constant punch and mandrel velocity of 15 mm/s.

Boundary conditions at the tool-workpiece interfaces were defined using the shear friction model with a coefficient of $m = 0.12$. The heat transfer coefficient was set to 5000 W/(m² K) to account for the thermal exchange between all components during the process. Both the friction and heat transfer coefficients represent established default values for the realistic representation of cold extrusion processes. These parameters provide a reliable basis for the current numerical investigation, yet experimental validation and specific adjustment of these values are planned for future research.

The discretization was performed using an adaptive meshing strategy to account for the varying workpiece segment volumes resulting from the different tooth numbers z of 16, 43 and 88. This strategy ensured a consistent minimum element length of 0.08 mm for all geometries by adjusting the total element count. Specifically, the workpiece segment for the gear with $z = 16$ had a total of 195.000 mesh elements, while the segments for $z = 43$ and $z = 88$ comprised 105.000 and 95.000 elements respectively. Local precision was enhanced by implementing a mesh window with a scaling factor of 0.1 in the toothing area while a global size ratio of 4 was maintained across all simulations. This approach was chosen to accurately model the material flow inside the tooth cavity while maintaining high computational efficiency. The complete set of simulation parameters is displayed in Table 1.

Regarding computational effort, simulations were performed on a workstation with an Intel Core i7 14700KF and 32 GB RAM. Average calculation times ranged from 4 to 6 hours while generating nearly 8 gigabytes of data per run. For the dataset of 450 simulations, this resulted in approximately 2250 hours of processing and 3.5 terabytes of storage. These demands highlight the necessity of the surrogate model for rapid and resource efficient optimisation.

Table 1. Simulation parameters for numerical Design of Experiment study.

Simulation parameter	Specification / Value
Software	Deform 3D™ - Version 14.0
Workpiece material	16MnCrS5
Workpiece material model	Ideally plastic
Mesh type	Tetrahedal mesh
Minimum element size of mesh	0.08 mm
Workpiece dimensions	D = 45 mm, d = 30 mm, h = 25 mm
Initial process temperature	20 °C
Friction model	Shear friction model, m= 0.12
Tool material model	Ideally rigid
Punch velocity	15 mm/s
Simulation type	Lagrangian incremental with heat transfer
Solver	Iterative Solver: Conjugate gradient
Iteration method	Direct iteration
Solution step definition	0.024 mm/step

Design of Experiments (DoE) Setup. A constrained Latin Hypercube Sampling (LHS) approach was employed to generate a representative and space-filling set of design parameters for the forming zone geometry. LHS was selected over factorial sampling methods to efficiently and uniformly cover the high dimensional space with a manageable number of simulations. The considered parameter space comprises the forming zone length L, the inlet radius R_1, the outlet radius R_2, the shoulder radius R_s, the undercut U and the cavity taper angle β (see Fig. 2b and Fig. 2c). The corresponding parameter ranges used for the sampling procedure are shown in Table 2.

Table 2. Parameter intervals used for Latin Hypercube Sampling with geometrical constraints of die design.

Parameter	Symbol	Unit	Minimum	Maximum
Forming zone length	L	mm	2.5	15
Inlet radius	R_1	mm	0.1	70
Outlet radius	R_2	mm	0.2	60
Shoulder curvature	*R-factor*	–	− 220.0	220.0
Undercut	U	–	0.1	0.8
Cavity taper angle	β	°	−5.5	5.5

Valid parameter boundaries were iteratively determined within the CAD environment to account for geometric constraints and ensure that all sampled configurations represent physically feasible die designs. The boundaries of the permissible parameter combinations were defined by envelopes derived from the iteratively determined dataset. Due to these constraints, the parameter ranges could not be evenly divided, but a modified LHS procedure was employed to achieve a quasi-uniform coverage of the design space. For this purpose, each parameter range was subdivided into intervals corresponding to the number of samples and the median value of each interval was selected and randomly permuted across samples. This approach ensured that all regions of the admissible parameter space were represented as evenly as possible while respecting geometric constraints. Dependent parameters such as the forming zone radius, the inlet radius and the undercut were assigned randomly within their allowable ranges, but always constrained to remain geometrically and technically feasible according to the CAD based dependency tables.

In addition to the forming zone geometry, the design of the tooth flank geometry was also considered. The design of experiments was performed separately for three different gear configurations:

- **Gear 1:** $z = 88$, $m = 0.5$ mm
- **Gear 2:** $z = 43$, $m = 1.0$ mm and
- **Gear 3:** $z = 16$, $m = 2.5$ mm

For each gear variant, an independent LHS was conducted and 150 design variants were generated and subsequently simulated. So, in total, 450 3D simulations were set up and performed.

Data extraction. The extraction of data from the numerical DoE focused on key process and geometric variables critical to the performance of the cold forging process and the gear quality. The evaluation targeted the punch force and the effective strain distribution at the tooth tip as an indicator for local strain hardening. Additionally, the die filling of the tooth and the resulting net gear height (see Fig. 4) were extracted as decisive parameters for the geometric feasibility and material efficiency of the cold forging process.

The extraction of results from the numerical DoE was executed through the DEFORM™ Application Programming Interface (API), which enabled a Python-based automated data acquisition. By utilising this approach, the punch force was acquired through the export of force-stroke data for each simulation variant. Parallel to the punch force data, local process variables were captured using a point tracking configuration. By positioning ten tracking points equidistantly at the workpiece mid-height, it was possible to record the radial displacement and effective strain along the gearing throughout the forming process. Regarding the strain analysis, the maximum value of effective strain recorded at the tooth tip tracking point was identified and utilised as the primary output for the subsequent training. The tooth underfilling was quantified by calculating the maximum radial displacement of the tracking point at the tooth tip from the defined tip circle diameter after the forming process was completed.

In order to evaluate available material efficiency, the final geometries were exported as '.GEO-files' and processed using a customised Python script. As illustrated in Fig. 5a, the analysis begins by extracting a point cloud along the symmetry plane of the gear tooth. For a robust evaluation across various geometries, the nodal data is transformed into a cylindrical coordinate system (r, z), allowing for a two-dimensional projection of the profile (see Fig. 5b).

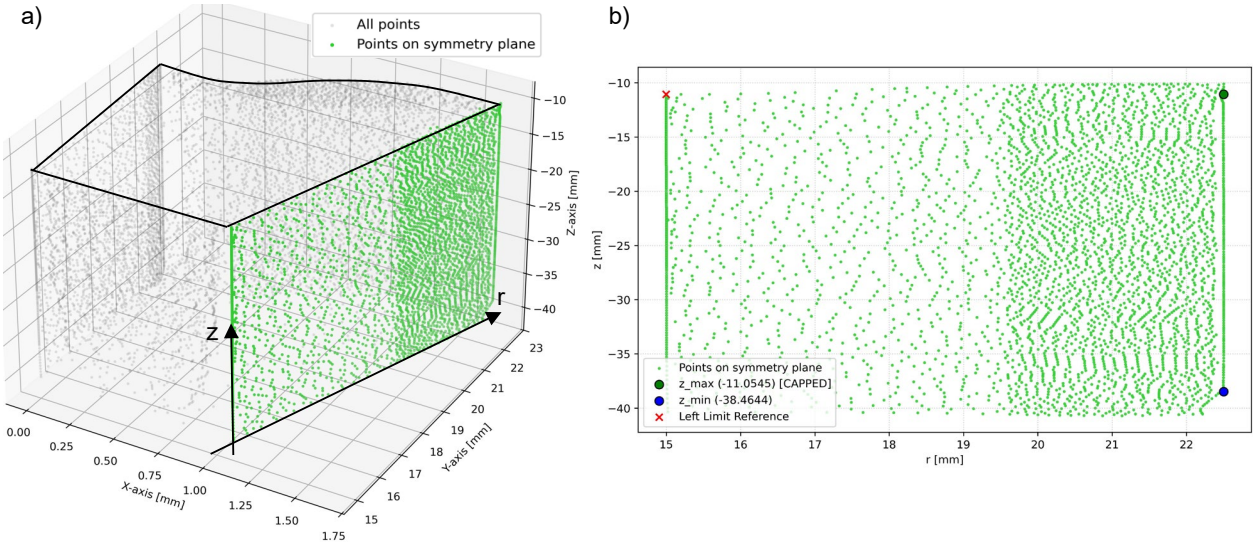

Fig. 5. Evaluation of net gear height: (a) '.GEO-point' cloud of gear wheel segment in cartesian coordinates gained from simulation; (b) 2D point cloud projected onto the r-z plane of the cylindrical coordinate system.

The assessment of die filling is performed at the maximum radial extension, which for the all gear configurations corresponds to a tip diameter of $r = 22.5$ mm. Within a defined tolerance of 0.05 mm, the algorithm identifies all nodes at this reference radius. Any radial displacement below this threshold is classified as underfilling. This way, the net gear height Δh is determined by performing a continuity check on the data points to identify connected segments of points within the defined tolerance, from which the geometric extrema $z_{\min}$ and $z_{\max}$ are extracted. An additional condition

ensures that if the detected z_{max} value exceeds the maximum height of deformation at the inner gear diameter (red cross in Fig. 5b), z_{max} is restricted to this inner height.

Data Processing and Gear-based Scaling

These steps are crucial to improve the numerical convergence of the machine learning algorithms and to ensure that the model accurately captures the influence of variations in the active die surface on the characteristics of the GMF process. The raw data extracted from the FE simulations requires systematic preparation to ensure high predictive accuracy and robust model performance. This section details the data processing pipeline and the scaling based on gear parameters applied to the input features and target variables, ensuring that the specific geometric properties of the gear teeth are appropriately represented in the model.

Gear-based Scaling. Numerical stability and scale-independence are achieved through a structured normalisation of the simulation data. This procedure ensures that the machine learning model prioritises geometric proportions over absolute dimensions. For this purpose, it was necessary to normalise the linear geometric parameters of the die's active surface by dividing them by the module m to generate dimensionless ratios. The shoulder radius used for designing linear, convex or concave shoulders, were normalized by the previously defined *R-factor* in Eq. 1. Normalising these geometric input parameters ensures that the data-based model evaluates the tools shape rather than its absolute size. Additionally, a gear-based scaling of the maximum punch force F_{max} by the product of the tooth number z and the squared module m^2, as shown in Eq. 2, was necessary:

$$F_{\mathrm{max,n}} = \frac{F_{\mathrm{max}}}{z \cdot m^2} \tag{2}$$

Scaling of the punch force is required to account for the varying projected deformation areas associated with different gear geometries, which fundamentally determine the resulting process load. In order to make the results comparable across different gear sizes, two scaling effects must be considered. First, the module m determines the size of an individual tooth; since the cross-sectional area grows quadratically as the module increases, a quadratic adjustment (m^2) is required. Secondly, the number of teeth z specifies the number of these individual sections that are formed simultaneously. By dividing the punch force data by $z \cdot m^2$, the value is effectively reduced to a specific load per unit area. This transformation allows the machine learning model to recognise that the underlying physics remains consistent, regardless of whether a small or large gear is produced. Thus, all three gear sizes can be calculated within the same model.

Surrogate Modelling Methodology

A data-driven modeling methodology was developed to map the complex interdependencies between the normalised tool geometry and the resulting forging parameters. A hybrid modeling approach was implemented, which combines a broad dataset from a Design of Experiments (DoE) with additional specific numerical reference cases (such as z = 60, m = 2 mm), hereafter referred to as anchor data points. This hybrid strategy ensures that the surrogate models benefit from the wide-ranging exploration of the design space while maintaining strict consistency at critical reference geometries and scale boundaries. Consequently, the methodology enables the reliable prediction of gear geometries with tip circle diameters that extend beyond the d_a = 45 mm constraint targeted for experimental validation in this study.

Model Generation and Training Strategy. The training process was conducted using the AutoGluon framework, employing an Automated Machine Learning (AutoML) strategy. To prioritise predictive performance, the ‘best_quality’ preset was selected, with a fixed training time of 3600 seconds assigned per model. To maximise predictive stability, the methodology utilises a Stacked Ensemble approach, training diverse model families, including Gradient Boosted Decision Trees (XGBoost, CatBoost, LightGBM) and Deep Neural Networks, in parallel.

A central challenge in surrogate modeling for forging processes, especially for gear forging, is the reliable prediction across different scales, particularly when varying the module m and or tooth number z. While the normalised geometric parameters often remain within the interpolated range, the resulting process parameters, such as the maximum punch force, scale quadratically with the module. The training dataset was augmented with the aforementioned anchor data points to prevent poor extrapolation behavior across different size scales of the gear and to ensure consistency at the boundaries of the design space. These anchor points consist of additional numerical simulations for two distinct reference tool geometries based on tooth numbers $z = 30$ and $z = 60$. For each group, a randomised but fixed geometric configuration was selected to serve as a baseline. These configurations are summarised in Table 3, with the parameters specified for a reference module of 1.0 mm.

By scaling these fixed geometries across three discrete modules (0.5 mm, 1.0 mm, and 2.0 mm), the surrogate models are trained to distinguish between shape-dependent effects and pure size-dependent scaling laws. This approach ensures that the training data covers a significantly broader range of gear configurations (z and m) with tip circle diameters extending far beyond the 45 mm constraint of the primary DoE. An oversampling strategy was applied to these anchor points for the training of all surrogate models, including maximum punch force, tooth underfilling, effective strain on the tooth tip, and net gear height. This prioritization ensures the accurate learning of the scaling laws across the design space, effectively creating a hybrid model that combines broad-range DoE data with precise numerical references for scale transition.

Table 3. Geometric configuration for the anchor data points at reference module of 1 mm

Parameter	Symbol	Unit	Configuration z = 60	Configuration z = 30
Forming zone length	L	mm	10.373	9.83
Inlet radius	R_1	mm	1.0	1.0
Outlet radius	R_2	mm	1.0	9.57
Shoulder radius	R_S	mm	35.0	100.0
Scaled shoulder Radius	*R-factor*	–	-28.57 (convex)	-10.0 (convex/linear)
Undercut	U	–	0.08	0.8
Cavity taper angle	β	°	-5.0	1.18

Model Validation and Performance. The reliability of the surrogate models was ensured through a two-stage validation process:

First, an internal 10-fold cross-validation (bagging) was employed during the training phase. In this procedure, the dataset is partitioned into ten distinct subsets, where each subset serves as a validation set once while the remaining nine subsets are used for training. This iterative process allows for an "out-of-fold" assessment of model stability across the entire dataset. The final prediction is an aggregate of these ten models, which significantly enhances robustness and provides a cross-validated performance metric that is less sensitive to individual outliers.

Second, the predictive performance was rigorously evaluated by comparing the final ensemble outputs against an independent validation set consisting of 90 unseen data set (20 % of the total data set). In contrast to the augmented training data, this validation set consists of unique, non-duplicated FE-simulations to ensure an unbiased assessment of the generalization capabilities. It includes the randomised geometric variants from the initial DoE as well as the specific anchor point configurations for tooth numbers $z = 30$ and $z = 60$ at modules of 0.5 mm, 1.0 mm, and 2.0 mm. By including these diverse scales in the independent test set, the model performance was explicitly assessed under both interpolation and extrapolation conditions. The results confirm that the integration of physical scaling laws and anchor points enables the model to maintain high accuracy even at the edges of the design space. As shown in Table 4, the methodology demonstrates excellent accuracy across all target parameters.

Table 4. Predictive performance and error metrics of the surrogate models for the target process parameters

Target parameter	Symbol	R^2 score (Training)	R^2 score (Test)	RMSE
Maximum punch force (scaled)	$F_{max,n}$	0.9402	0.9367	0.1827
Tooth underfilling	Δr	0.9935	0.9836	0.0259
Effective strain on tooth tip	ε_{tip}	0.9778	0.9646	0.1879
Net gear height	Δh	0.9751	0.9491	3.7028

The high consistency between the cross-validated training scores and the independent test scores ($R^2 > 0.93$) confirms that the models successfully captured the underlying physical relationships without overfitting. For the geometry-related outputs, such as tooth underfilling (Δr) and net gear height (Δh), the training and test performances show nearly identical R^2 values, with scores of 0.9836 and 0.9491 on the test set, respectively. This indicates that the stacked ensemble of both models reached its maximum predictive stability for these continuous geometric correlations.

The small difference in accuracy for the maximum punch force ($F_{max,n}$) delivers a deliberate result of the oversampling strategy. By giving the anchor points more weight during training, the model is forced to follow the physical laws of gear scaling (or module scaling). This prevents the model from "smoothing out" important peaks in the data just to get a better statistical average. Although this leads to a slightly lower global R^2 score, it ensures that the model remains physically accurate and reliable even for very large or very small gear sizes at the edges of the design space.

As shown in Fig. 6 and Fig. 7, the feature importance analysis identifies the forming zone length (L) as the most significant factor across all four surrogate models.

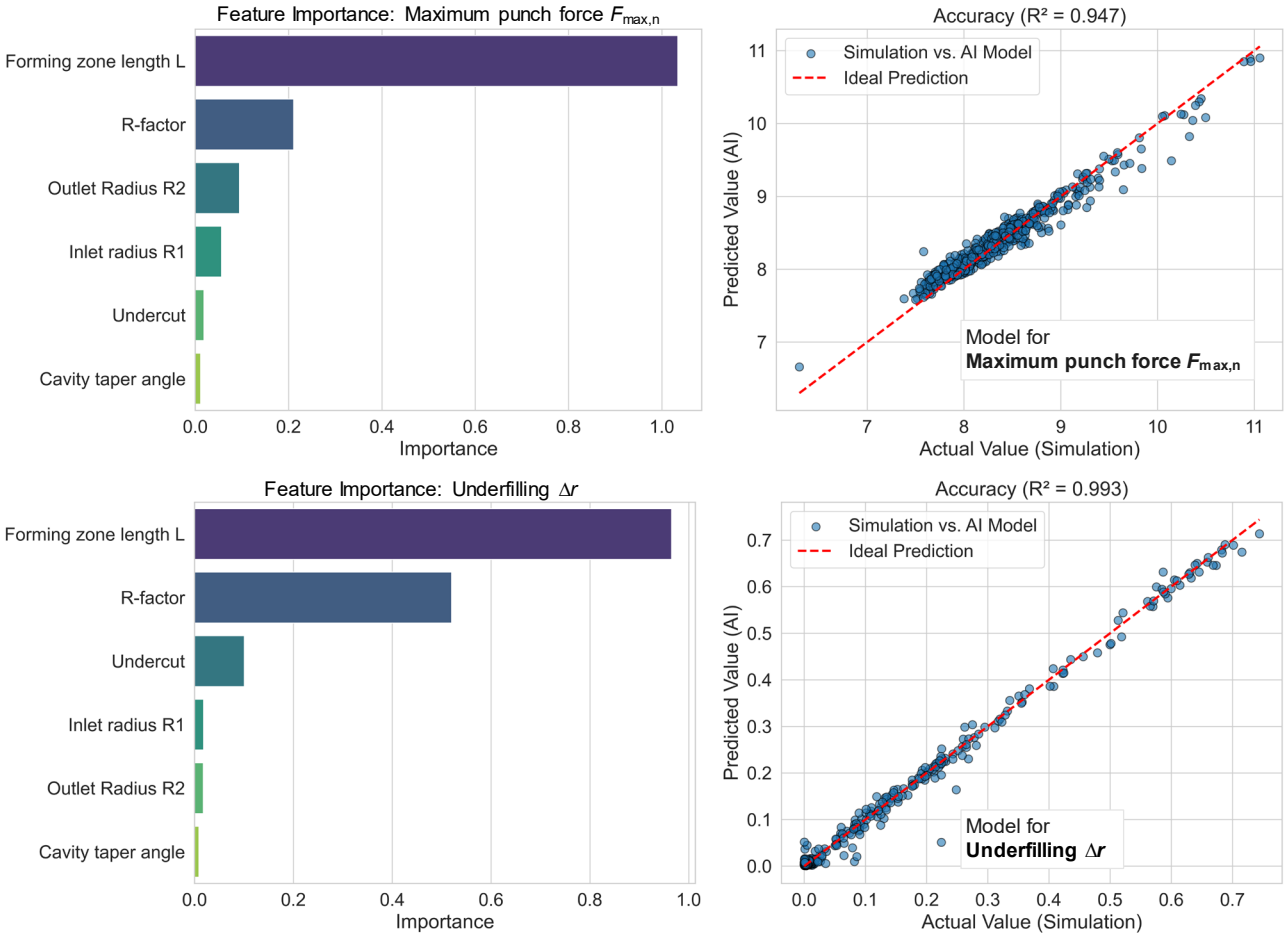

Fig. 6. Evaluation of feature importance and model performance of the surrogate models for punch force and underfilling prediction

The dominant influence of the forming zone length L on tooth underfilling and effective strain demonstrates that this axial dimension is the main driver for material flow and geometric accuracy. The *R-factor*, which defines the curvature of the extrusion shoulder, is the second most important feature for net gear height and underfilling. This reflects how sensitive the material flow and the subsequent cavity filling are to the geometry of the transition zone where the radial material displacement occurs.

In contrast, the cavity taper angle has almost no impact on the process outputs within the tested range. This suggests that the primary dimensions of the forming zone are far more important for the forging results than the slight tapering angle of the tooth cavity. The scatter plots in Fig. 6 and Fig. 7 show that the validation data points lie very close to the ideal diagonal line. Combined with the low RMSE values, this confirms that the developed methodology is a reliable and fast replacement for expensive FE-simulations in the design of dies for the GMF process.

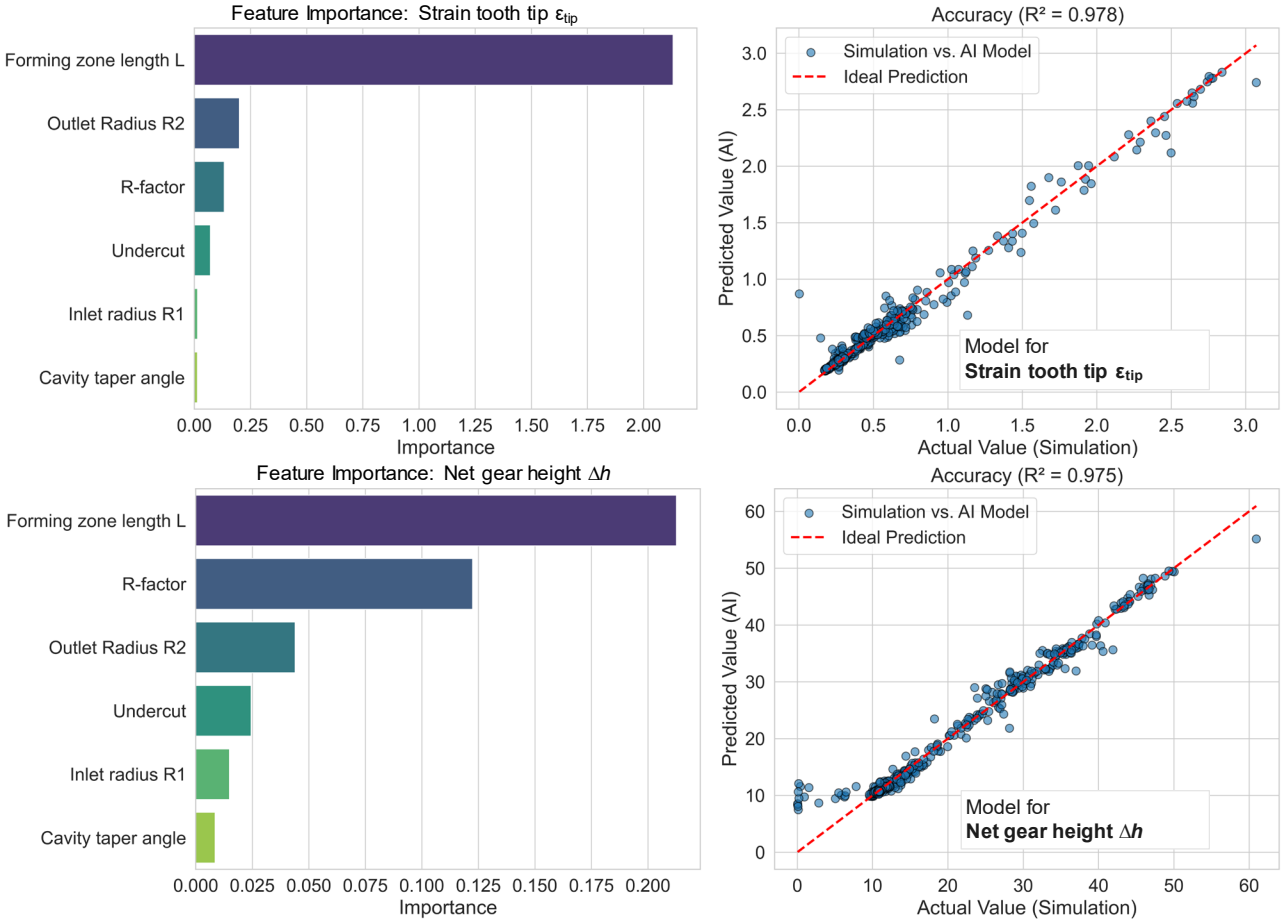

Fig. 7. Evaluation of feature importance and model performance of the surrogate models for strain and net gear height prediction

Conclusion and Outlook

In the present study, a hybrid surrogate modeling approach was developed to predict the process parameters and geometric outcomes of the Guided Material Flow (GMF) process. The core of this methodology lies in the integration of a broad-range numerical Design of Experiments (DoE) with targeted, oversampled anchor points. These anchor points significantly extend the model's operational range by incorporating gear configurations with pitch and tip circle diameters that considerably exceed the initial 45 mm constraint of the primary numerical DoE. This strategy effectively overcomes the inherent extrapolation limitations of conventional meta-models and ensures physical consistency across a wide spectrum of gear dimensions.

The developed models provide a profound understanding of the GMF process, enabling the user to systematically influence and control forging results according to specific requirements, such as the reduction of maximum punch force or the enhancement of material utilization. The high predictive accuracy (R^2>0.93) and the sensitivities identified through feature importance analysis demonstrate that the surrogate models reliably capture the complex non-linear correlations of this cold forging operation.

Future research will focus on the development of a multi-objective optimization framework based on these validated surrogate models. By using a weighted objective function, the system will allow users to find the best tool geometry for a given task. Specifically, this framework will be used to identify tool designs that minimise tool loads and maximise filling quality. This development represents a significant advancement toward the cold forging of gears with lower tool stress and, consequently, higher dimensional accuracy of the forged components.

Acknowledgments

The authors would like to thank the Deutsche Forschungsgemeinschaft (DFG) for the financial support of the research project "Cold forging of gears with targeted reduction of friction surfaces – Guided Material Flow (GMF) process" under the project number LI 1556/80-1.

DFG Deutsche Forschungsgemeinschaft

References

[1] K. Lange, M. Kammerer, K. Pöhlandt, and J. Schöck, Fließpressen: Wirtschaftliche Fertigung metallischer Präzisionswerkstücke: Springer, 2008.

[2] M. Merklein, C. Kiener, and A. Reiss, "Numerical Investigations on the Influence of Process Parameters on the Forming of Gears in Forward Extrusion," *AMM*, vol. 805, pp. 154–161, 2015, doi: 10.4028/www.scientific.net/AMM.805.154.

[3] J. Choi, H. Cho, and H. Kwon, "A new extrusion process for helical-gears: experimental study," *Journal of Materials Processing Technology*, vol. 44, no. 1, pp. 35–53, 1994, doi: 10.1016/0924-0136(94)90036-1.

[4] Z. Liu, Q. Wang, J. Zhou, W. Feng, and Q. Liang, "Design of precision finishing method for cold extruded sun gear with internal-external tooth shapes," *Int J Adv Manuf Technol*, vol. 116, 9-10, pp. 3277–3293, 2021, doi: 10.1007/s00170-021-07477-6.

[5] W. Wang and J. Zhao, "Application of Open-die Warm Extrusion Technique in Spur Gear Manufacturing," in *Extrusion of Metals, Polymers and Food Products*, S. Z. Qamar, Ed.: InTech, 2018.

[6] C. Kiener and M. Merklein, "Researching of commonalities and differences in cold forging of spur and helical gears," *Prod. Eng. Res. Devel.*, vol. 13, 3-4, pp. 391–397, 2019, doi: 10.1007/s11740-019-00887-2.

[7] C. Kiener, K. Andreas, and M. Merklein, "Basic Numerical Analysis of a “Samanta” Based Forward Extrusion Process," *AMR*, vol. 1140, pp. 27–34, 2016, doi: 10.4028/www.scientific.net/AMR.1140.27.

[8] C. Kiener, "Kaltfließpressen von gerad-und schrägverzahnten Zahnrädern," Dissertation, Lehrstuhl für Fertigungstechnologie, Friedrich-Alexander-Universität Erlangen-Nürnberg, 2020.

[9] S. Samanta, "Apparatus and method for cold extrusion of gears," USA United States Patent 1191 1111 3,910,091.

[10] S. Samanta and M. Ypsilanti, "Verfahren und Einrichtung zum Herstellen von Zahnrädern," DE 25 33 670.

[11] A. Schwager, M. Kammerer, K. Siegert, A. Felde, E. Körner, and V. Szentmihalyi, "Cold Forming of Helically Internal Toothed Wheels," *New Developments in Forging Technology*, pp. 489–503, 2003.

[12] A. Weiß, T. Deliktas, M. Liewald, and N. Missal, "Cold forging of gear components by a modified Samanta process," *Forschung im Ingenieurwesen*, no. 3, pp. 215–221, 2020, doi: 10.1007/s10010-020-00403-4.

[13] T. Deliktas and M. Liewald, "Numerical study on cold extrusion of gears varying the extrusion shoulder geometry: Material Forming - ESAFORM 2023," *Materials Research Proceedings*, vol. 28, 2023.

[14] A.Schenek, "Surrogat-Modelle zur Auslegung und Optimierung einhubiger Scherschneidprozesse," Dissertation, Institute for Metal Forming Technology, University of Stuttgart, 2024. [Online]. Available: https://nbn-resolving.de/urn:nbn:de:bsz:93-opus-ds-153761